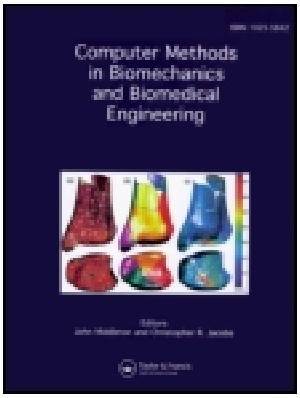

Computer Methods in Biomechanics and Biomedical Engineering
Publication details, including instructions for authors and subscription information:
http://www.tandfonline.com/loi/gcmb20

A modified human head model for the study of impact head injury

Wenyi Yan [a] & Oscar Dwiputra Pangestu [a]

[a] Department of Mechanical and Aerospace Engineering, Monash University, Clayton, VIC, 3800, Australia

Available online: 24 May 2011

Computer Methods in Biomechanics and Biomedical Engineering
Vol. 14, No. 12, December 2011, 1049–1057

A modified human head model for the study of impact head injury

Wenyi Yan* and Oscar Dwiputra Pangestu

Department of Mechanical and Aerospace Engineering, Monash University, Clayton, VIC 3800, Australia

(*Received 20 March 2010; final version received 2 July 2010*)

A recently published finite element (FE) head model is modified to consider the viscoelasticity of the meninges, the spongy and compact bone in the skull. The cerebrospinal fluid (CSF) is simulated explicitly as a hydrostatic fluid by using a surface-based fluid modelling method, which allows fluid and structure interaction. It is found that the modified model yields smoother pressure responses in a head impact simulation. The baseline model underestimated the peak von Mises stress in the brain by 15% and the peak principal stress in the skull by 33%. The increase in the maximum principal stress in the skull is mainly caused by the updation of the material's viscoelasticity, and the change in the maximum von Mises stress in the brain is mainly caused by the improvement of the CSF simulation. The study shows that the viscoelasticity of the head tissue should be considered, and that the CSF should be modelled as a fluid, when using FE analysis to study head injury due to impact.

Keywords: finite element modelling; impact head injury; cerebrospinal fluid; viscoelasticity

1. Introduction

1.1 Anatomy of human head

The human head consists of three main layers surrounding and protecting the brain, as illustrated in Figure 1. The three layers in descending order are the scalp, skull and meninges. The outermost layer, the scalp, is 3–6 mm thick and can be further subdivided into five sub-layers: skin with hairy coverings, tela subcutanea, which connects the skin to the next sub-layer, the aponeurotic sub-layer consisting of flattened tendon, the subaponeurotic sub-layer and the pericranium, which connects the whole scalp to the skull. The skull is 9.5–12.7 mm thick. It consists of a layer of spongy bone (trabecular bone) sandwiched between two layers of compact bone (cortical bone). The third layer, the meninges, is about 2.5 mm thick and is composed of three sub-layers: the dura mater, arachnoid mater and pia mater. The dura and arachnoid mater are separated by a space called subdural space, while the arachnoid and pia mater are separated by another space called the subarachnoid space. In this subarachnoid space, there is string-like tissue called arachnoid trabeculae, which connects arachnoid to pia mater. Within the subarachnoid space, there is also water-like fluid called cerebrospinal fluid (CSF), which provides damping and cushions for the brain under impact situations.

CSF is produced within the brain, the innermost part of the human head. The outer layer of the brain is made of grey mater forming a 1.5–3.5-mm thick cortex with an irregular shape, consisting of numerous ridges, called gyrus, and depressions, called sulcus. The inner layer of the brain is made of another tissue called white mater, and in the centre of this inner layer lies four ventricles, which are the sources for the CSF. The brain can also be divided into three regions: the cerebrum, cerebellum and brainstem. The cerebrum and cerebellum are separated by a fold of dura mater, called tentorium cerebelli, and can be further divided into the left and right hemisphere by another fold of dura, called falx cerebri and falx cerebelli. These folds of dura have similar layers and components to those of the meninges. In addition, numerous small to large blood veins and arteries spread across the human head, which are often neglected in theoretical studies of impact head injury. The large blood veins are found inside the dural sinuses.

1.2 Modelling of head impact

Head injury due to impact is a common human body injury, which can have serious consequence and even death. Various attempts have been made to investigate impact head injury. These include cadaver and animal studies, physical modelling, mathematical modelling and numerical finite element (FE) modelling.

Two extensive cadaver studies were performed by Nahum et al. (1977) and Trosseille et al. (1992). Nahum et al. performed a series of blunt impacts on stationary unembalmed cadavers. The Frankfort anatomical plane of these cadavers was inclined at 45° to the horizontal, and the impact condition was generated by hitting a 5.59 kg impactor at a speed of 9.94 m/s to the frontal head. The impact was directed right through the centre of mass of the

*Email: wenyi.yan@eng.monash.edu.au

ISSN 1025-5842 print/ISSN 1476-8259 online

http://dx.doi.org/10.1080/10255842.2010.506435
http://www.tandfonline.com

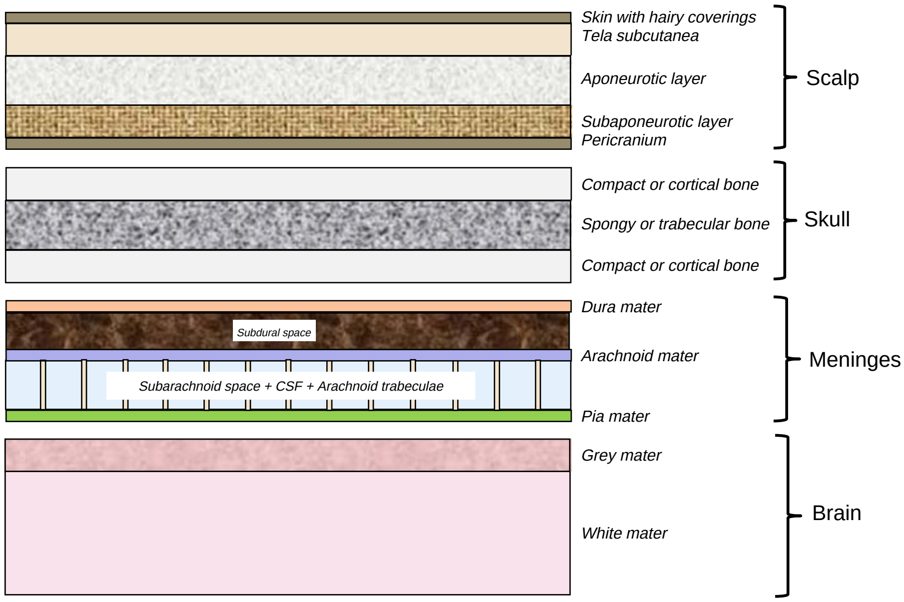

Figure 1. Illustration of human head layers surrounding the brain.

head so that a purely translational impact was achieved. Five pressure transducers were inserted into the subdural space at the frontal area adjacent to the impact point, in order to record the intracranial pressure. The transducers were located above the coronal and squamosal suture in parietal area, below the lambdoidal suture in occipital area and posterior fossa. The resulting pressure time histories from Nahum et al.'s study have been widely used as a validation to various physical, mathematical and FE models (Zhou et al. 1995; Willinger et al. 1999; Kleiven and Holst 2002; Horgan 2005). Trosseille et al. (1992) conducted a study similar to that of Nahum et al., in which six cadavers were impacted by a 23.4-kg impactor at 7 m/s. The impact, however, did not pass through the centre of mass of the head so that a combination of rotational and translational impact was generated. Due to its precise geometry and material properties, cadaver studies have been preferred as a means of validation to physical, mathematical and FE models.

Anaesthetised animals are often substituted for cadavers. The differences in geometry and material properties, however, have been the main limitations in performing this type of study. It was proposed that a certain scaling is required to match the animal results to human results (Margulies et al. 1985). Regardless, animal studies are still useful to determine the main trend and mechanism behind brain injuries. A study conducted on monkeys by Pudenz and Shelden (1946) showed that the brain motion lagged behind the skull upon impact, causing what is called countercoup injury. This is in line with results obtained by Nahum et al. (1977), in which a large hydrostatic pressure was observed at the coup site and a large negative pressure was observed at the countercoup site. In addition, Pudenz and Shelden (1946) observed a larger lag of brain motion when the CSF layer from one monkey was removed, thus demonstrating the damping effect of the CSF layer.

Cadaver and animal studies are limited by their non-repeatability due to variances in dimensions and material properties. Therefore, physical models are developed to allow repeatable simulations. Gurdjian (1972) conducted a study using a water-filled physical model that correlates well with the results obtained by Pudenz and Shelden (1946), in which high pressure was observed near the impact site and large negative pressure at the countercoup site. Margulies et al. (1985) used their model to investigate the scaling of animal studies to that of human. The results showed good correlation with previous experimental work conducted using baboon heads.

Mathematical models, in contrast to other forms of modelling, offer excellent repeatability and consistency. The most recent mathematical modelling technique is the FE method, which utilises computational power to simultaneously break down and solve the displacement response of a finite number of defined elements in a model. FE models can simulate the complexity of the human head structure and real impact loading conditions. Additionally, the local stress and strain state in any part of the human head during an impact process, which is almost impossible to be obtained from an experimental test, can be an output from an FE impact simulation. From a biomechanics point of view, the local stress in the brain will determine the extent of the brain injury, while the local stress in the skull will determine whether the skull will fracture. For these reasons, FE modelling has been playing an increasing role in the study of impact head injury. To date, various FE models have been developed, e.g. Ruan et al. (1991), Zhou et al. (1996) and Willinger et al. (1999). The most recent model was developed by Horgan and Gilchrist (2003, 2004) using CT-data from the National Institute of Health to construct a 3D head model of an adult male with excellent precision.

Simplifying assumptions are often made in order to develop FE head models. In Horgan and Gilchrist's model, the CSF was simplified as a low shear modulus solid, which is prone to excessive distortion and unnatural resistance under large skull–brain displacement (Couper and Albermani 2007). Except the brain, all tissues were treated as linear elastic materials (Horgan 2005).

The aim of this study is to improve Horgan and Gilchrist's existing model by including viscoelasticity in the material definition of all the tissues. The CSF will be modelled as a hydrostatic fluid using a surface-based method, which is able to model fluid and structure interaction without the need of any elements, thus avoiding excessive distortion and unnatural resistance.

2. Model development

2.1 Horgan and Gilchrist's model

Horgan and Gilchrist's model (subsequently referred as the 'baseline model') is available on the Internet through the BEL repository managed by the Istituti Ortopedici Rizzoli, Bologna, Italy (Available from: http://www.biomedtown.org/biomed_town). The model comprises three main layers surrounding the brain: the scalp, the skull and the meninges, as shown in Figure 2. The scalp is modelled using single-layer shell elements, which have combined material properties of the five sub-layers found in the actual human head. This scalp is 5 mm thick and is assumed to be linear elastic with an elastic modulus of 16.7 MPa and Poisson's ratio of 0.42.

The skull is modelled using brick elements and comprises a layer of spongy (trabecular) bone sandwiched between two layers of compact (cortical) bone. The compact and spongy bone has a varying thickness of approximately 2.5 and 5 mm, respectively. Again, these materials are assumed to be linear elastic: with an elastic modulus of 15 GPa and Poisson's ratio of 0.22 for the compact bone; and an elastic modulus of 1 GPa and Poisson's ratio of 0.24 for the spongy bone. Furthermore, the facial bone is also modelled using shell elements with an elastic modulus of 5 GPa and Poisson's ratio of 0.23.

The arachnoid mater, arachnoid trabeculae and subdural space are not modelled in the baseline model. The dura mater is modelled using shell elements, and it is 1 mm thick with an elastic modulus of 31.5 MPa and Poisson's ratio of 0.45. Membrane elements are used to model the pia mater, which is 0.5 mm thick and has an elastic modulus of 11.5 MPa and Poisson's ratio of 0.45. The subarachnoid space is approximately 1.3 mm thick (varying throughout the model) and only occupied by CSF. The CSF is modelled as a solid; using brick elements, with an elastic modulus, bulk modulus and Poisson's ratio of 0.15 MPa, 2.273 GPa and 0.499989, respectively.

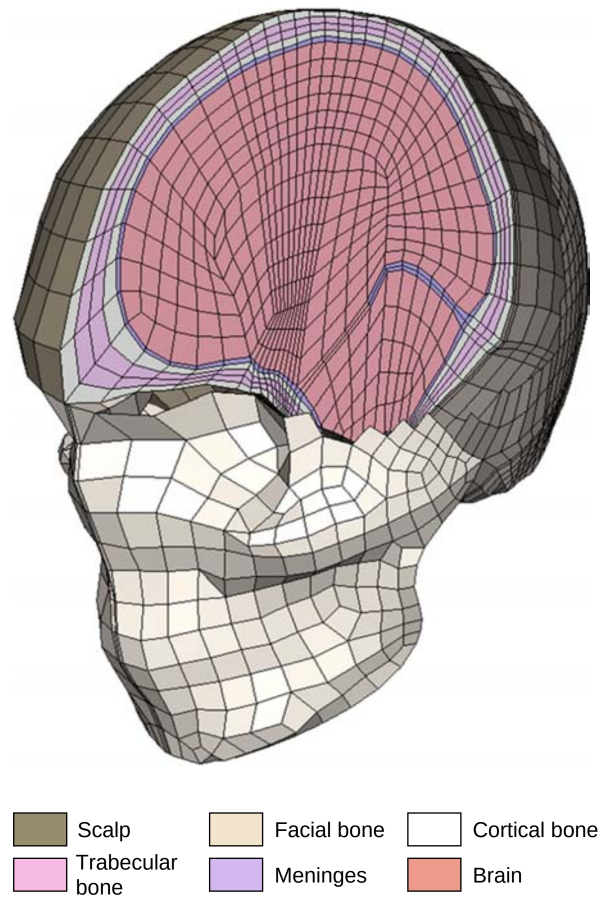

Figure 2. A cutting view of the baseline and the modified model. Note that the sub-layers of the meninges are not shown due to their small thickness.

Brick elements are used to model the combined properties of the grey and white matter of the brain. The long-term elastic modulus, bulk modulus and Poisson's ratio are 22.8 kPa, 2.278 GPa and 0.499991, respectively. In terms of viscoelasticity, the relaxation (current) shear modulus $G_R(t)$ is determined by the following dimensionless function, $g_R(t)$, expressed as a Prony series (Abaqus 2008):

$$g_R(t) = 1 - 0.8150 \times (1 - e^{-t/0.00143}), \qquad (1)$$

where $g_R(t) = G_R(t)/G_0$, and G_0 is the instantaneous shear modulus. When the time t takes an infinite value, the long-term shear modulus can be obtained from the Prony series as

$$G_\infty = G_R(\infty) = g_R(\infty) \times G_0. \quad (2)$$

The elastic modulus E, the shear modulus G and Poisson's ratio v, at any time, are related by the following well-known relationship:

$$G = \frac{E}{2(1+v)}. \quad (3)$$

The bulk modulus K is determined by

$$K = \frac{E}{3(1-2v)}. \quad (4)$$

According to Horgan (2005), Equation (1) was obtained by Zhou et al. (1996) from the frequency test data of Shuck and Advani (1972). Furthermore, the baseline model also comprises some of the dura folds (tentorium cerebelli and falx cerebri only), which have the same components and properties as the meninges. The dural sinuses and all blood vessels are not modelled.

2.2 *Modified model*

The modified model also has three main layers surrounding the brain: the scalp, the skull and the meninges. A cutting view of the baseline and the modified model is shown in Figure 2. We are not able to find the reliable viscoelastic properties of human scalp. Numerical tests indicated that the treatment of the scalp as a linear elastic or viscoelastic material does not affect the impact simulation results. Therefore, the scalp definition was unchanged in the modified model.

The compact bone was simulated as a linear viscoelastic material. Due to the lack of experiment studies on the viscoelastic properties of the compact bone of the skull, experimental data of the compact bone of a human tibia, obtained by Lakes et al. (1979), were applied in this study. Using the published shear modulus data from Lakes et al. (1979), curve fitting was applied to determine the Prony series approximation for relaxation (current) shear modulus, which is shown in Table 2. The spongy bone was also treated as a viscoelastic material and the material data were obtained from Yue et al. (2008), as shown in Table 2.

In the modified model, the thickness of the dura mater was reduced to 0.4 mm, according to the results from Bashkatov et al. (2003). The viscoelastic properties of the dura mater were obtained from Yue et al. (2008), and are shown in Table 2. Arachnoid mater and trabeculae were added to the model as shell (0.35 mm thick) and beam elements (Ma et al. 2008), respectively. Their elastic moduli (long-term) were defined to be 19.32 and 0.055 MPa, respectively, with identical Poisson's ratio of 0.45. The pia mater was modelled using shell elements, with the thickness reduced to 0.15 mm, the long-term elastic modulus increased to 19.32 MPa, and Poisson's ratio unchanged. The dimensionless relaxation moduli of the arachnoid mater, trabeculae and pia mater are listed in Table 2 (Ma et al. 2008).

The CSF was simulated as a hydrostatic fluid filled in cavities by using a surface-based fluid modelling method (Abaqus 2008). This method uses a surface definition to provide the coupling between the deformation of the fluid-filled structure and the pressure exerted by the contained fluid on the cavity boundary of the structure. It excels in its ability to model the fluid and structure interaction without the need of any elements, thus preventing excessive distortion and unnatural resistance that could be associated with an element-based method. The CSF-filled space was subdivided into 163 hydrostatic fluid cavities. It was expected that modelling the CSF space as numerous hydrostatic fluid cavities would imitate the pressure variations in CSF during a dynamic impact. Furthermore, the bulk modulus of the CSF was taken as 22 MPa, in accordance with the model detailed by Zhou et al. (1995).

Based on the study carried out by Zhou et al. (1996), the long-term elastic modulus of the brain was specified as 22.8 kPa. Instead of using a Prony series, the original frequency test data from Shuck and Advani (1972) were used directly to describe the viscoelastic behaviour of the brain. The material properties of the baseline and the modified model are summarised in Tables 1 and 2, respectively.

3. Results and discussion

To check the improvement of the modified head model, both the modified and Horgan and Gilchrist's models were applied to simulate Nahum et al.'s (1977) impact experiment. According to Horgan (2005), the long-term elastic modulus of the brain was adjusted to 22,800 Pa in the downloaded model from the Internet (Available from: http://www.biomedtown.org/biomed_town).

According to the experiment by Nahum et al. (1977), the Frankfort plane of the head was inclined at 45° to the horizontal prior to the impact, as illustrated in Figure 3. The impact condition was generated by inputting force amplitude as a function of time to a rigid impactor. This force amplitude curve was obtained from the impact force data reported by Nahum et al. (1977), which is shown in Figure 4. It is evident that the recorded impact lasted about 0.015 s, and the largest impact force occurred at around 0.004 s. The pressure response at the coup, countercoup and occipital region can be plotted during the impact process, and can be used to compare the results predicted by the numerical models with the experimental data presented by Nahum et al. (1977). The pressure response

Table 1. Material properties of the baseline model.

Layer	Sub-layer	Behaviour	Thickness (mm)	Density (kg/m^3)	Elastic modulus (MPa)	Bulk modulus (MPa)	Poisson's ratio	Viscoelastic response (Prony series approximation)
Scalp	Skin Tela subcutanea Aponeurotic layer Subaponeurotic layer Pericranium	Elastic	5.00	1130	16.700	35	0.42	–
Skull	Compact bone	Elastic	2.50	2000	15,000	8929	0.22	–
	Spongy bone	Elastic	5.00	1300	1000	641	0.24	–
	Facial bone	Elastic	10.00	2500	5000	3086	0.23	–
Meninges	Dura mater	Elastic	1.00	1140	31.500	105	0.45	–
	CSF	Elastic	1.30	1000	0.150	2273	0.499989	–
	Pia mater	Elastic	0.50	1130	11.500	38	0.45	–
Brain	Grey mater White mater	Viscoelastic	–	1040	0.0228 (Long term)	2278	0.499991	$g_R(t) = 1 - 0.8150\,e^{-t/70.00143}$

Table 2. Material properties of the modified model.

Layer	Sub-layer	Behaviour	Thickness (mm)	Density (kg/m^3)	Long-term elastic modulus (MPa)	Bulk modulus (MPa)	Poisson's ratio	Viscoelastic response (Prony series approximation)
Scalp	Skin Tela subcutanea Aponeurotic layer Subaponeurotic layer Pericranium	Elastic	5.00	1130	16.700	35	0.42	–
Skull	Compact bone	Viscoelastic	2.50	2000	13,000	7738	0.22	$g_R(t) = 1 - 0.0293(1 - e^{-t/9}) - 0.0656(1 - e^{-t/950}) - 0.0278(1 - e^{-t/9500}) - 0.107(1 - e^{-t/90,000})$
	Spongy bone	Viscoelastic	5.00	1300	888	740	0.30	$g_R(t) = 1 - 0.6224(1 - e^{-t/711.23}) - 0.2143(1 - e^{-t/4267.4})$
	Facial bone	Elastic	10.00	2500	5000	3086	0.23	–
Meninges	Dura mater	Viscoelastic	0.40	1140	11.720	7	0.23	$g_R(t) = 1 - 0.1088(1 - e^{-t/40}) - 0.0959(1 - e^{-t/10,000}) - 0.0922(1 - e^{-t/10,00,000})$
	Arachnoid mater	Viscoelastic	0.35	1130	19.320	64	0.45	$g_R(t) = 1 - 0.9190(1 - e^{-t/0.002})$
	CSF	Fluid	1.30	1000	–	22	–	–
	Arachnoid trabeculae	Viscoelastic	–	1130	0.050	0.17	0.45	$g_R(t) = 1 - 0.8282(1 - e^{-t/0.01})$
	Pia mater	Viscoelastic	0.15	1130	19.320	64	0.45	$g_R(t) = 1 - 0.9190(1 - e^{-t/0.002})$
Brain	Grey mater White mater	Viscoelastic	–	1040	0.123	2278	0.499998274	Frequency test data from Shuck and Advani (1972)

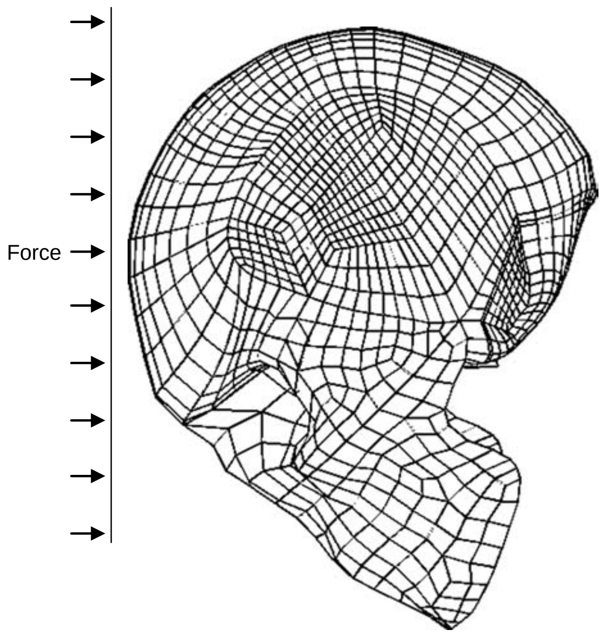

Figure 3. Illustration of the impact direction in our numerical simulations.

was taken from subarachnoid space, since it is closer to the subdural space where the actual pressure response was measured by Nahum et al. (1977). Figure 5 illustrates the locations where the pressure was obtained from the numerical simulations in this study. The effects of the modification to the baseline model on the intracranial pressure response, the maximum principal stress in the skull and the maximum von Mises stress in the brain will be discussed below.

3.1 Intracranial pressure response

Figure 6 shows the intracranial pressure at different locations, as predicted by the baseline and modified

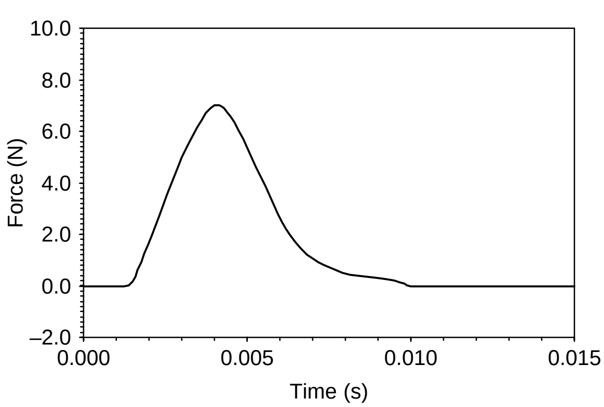

Figure 4. Impact force history recorded from experiment number 37 by Nahum et al. (1977), which is applied on the rigid impactor in our FE simulations.

numerical models and obtained from experimental testing (Nahum et al. 1977). Both the models predict the same distribution trend for the pressure as shown by the experimental results at each of the four positions. The pressure at the coup position is the major concern in experimental head impact tests; see Figure 6(A). Both models overestimated the maximum pressure at the coup position, and the time at which the corresponding maximum pressure is reached is also different from the experimental datum. These differences are caused by the fact that the dimensions of the head models are different from that of the head used in the experiments by Nahum et al. (1977). Horgan and Gilchrist (2003) achieved a better agreement by modifying the dimensions of their model to match those used by Nahum et al. (1977). As shown in Figure 6(A), the maximum pressure predicted from the modified model is 17 kPa less than that from the baseline model. It is evident that the baseline model predicted an oscillated pressure response at the beginning and end of the impact with some negative pressure values. This type of behaviour seems unreasonable, based on the experimental results shown. The modified model has almost removed this oscillation and provided a smoother and more rational pressure distribution.

3.2 The maximum von Mises stress in the brain

One of the main reasons for developing an FE head model is to apply it to investigate impact head injury. The value of von Mises stress has been used to examine the brain injury risk; for example, see Marjoux et al. (2008). Therefore, the maximum von Mises stress in the brain at any moment during the impact simulations was output from the numerical models, which was examined in further detail, as shown in Figure 7. Both models predict the same trend of the maximum von Mises stress distribution in the brain during the whole impact process, with the time at which the peak values occurred corresponding to that of the peak impact force. However, the peak values are significantly different. It is evident that the peak von Mises stress predicted in the baseline model is approximately 15% lower (from 29.56 to 25.16 kPa) than that in the modified model. Therefore, when applying it to evaluate the brain injury in a real situation, the baseline model can significantly underestimate the brain damage risk (see Marjoux et al. 2008). In the modified model, the CSF has been simulated directly as a fluid, not a solid. Additionally, the viscoelastic properties of the head materials have been considered in the modified model. For these reasons, it is likely that the stresses predicted from the modified model are more accurate than those from the baseline model.

3.3 The maximum principal stress in the skull

With regard to head skull fracture due to impact, the maximum principal stress in the skull is considered as the

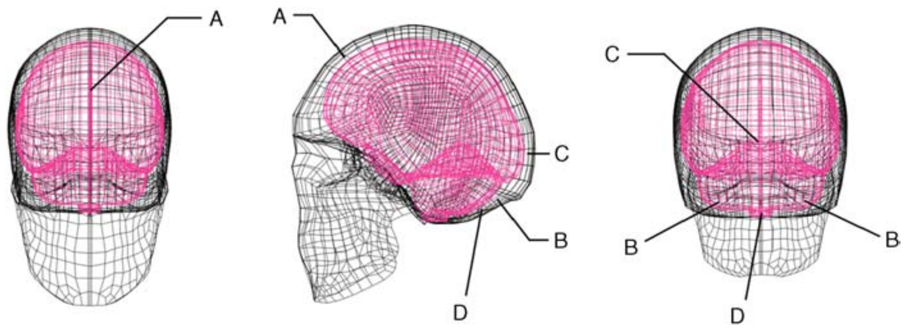

Figure 5. Locations for obtaining pressure in both baseline and modified models. Coup position is marked by (A), countercoup position by (D) and upper and lower occipital positions by (C) and (B), respectively.

suitable variable to evaluate the situation; for example, refer to Yoganandan and Pintar (2004). Figure 8 shows the maximum principal stress predicted to occur during the whole impact process, using the baseline and modified numerical models. The modifications increase the prediction of the peak principal stress in the skull by 48% from 17.2 to 25.5 MPa. Hence, it is likely that the baseline model underestimates the peak stress value by 33%, and, therefore, would significantly underestimate the skull fracture probability when applied to examine a real head impact.

Two modifications have been made in the new modified head model. Firstly, instead of assuming the CSF as a solid, it has been simulated as hydrostatic fluid cavities. Secondly, except for the scalp, all the head tissues are simulated as viscoelastic materials, which should result in improved predictions, compared to the original linear elastic material assumption. The individual effects of these two modifications, on the maximum von Mises stress in the brain, are shown in Figure 9. The dash-dotted curve is obtained from the model where only the modification to the CSF was made. As we can see, this modification alters

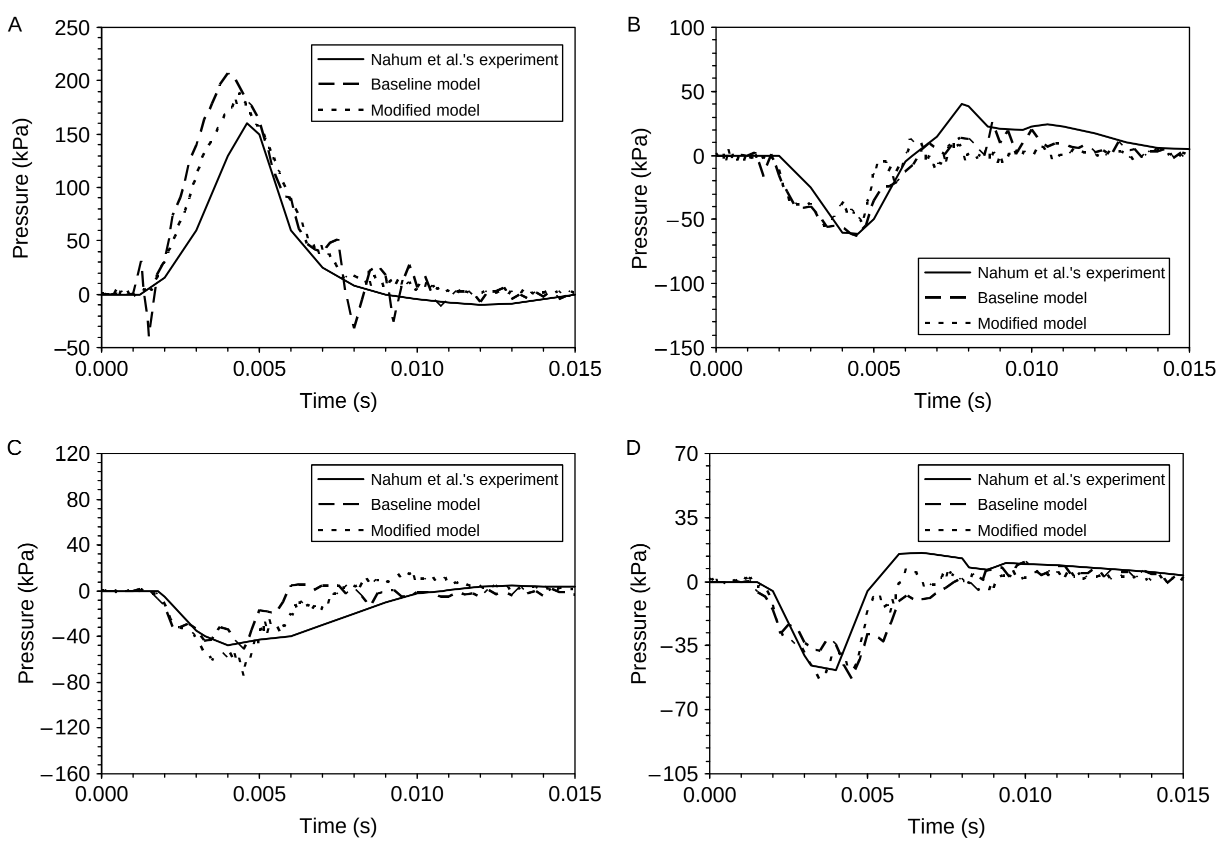

Figure 6. Subarachnoid pressure response from the baseline and modified models: (a) at coup position, (b) at coutercoup position, (c) at upper occipital position and (d) at lower occipital position.

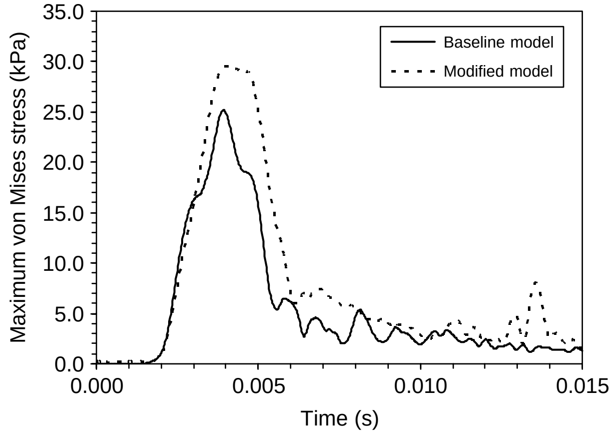

Figure 7. Predictions of the maximum von Mises stress in the brain during the impact process from the baseline and the modified models.

the maximum von Mises stress behaviour significantly from the baseline model (solid curve). Furthermore, it is evident that the dash-dotted curve is close to the dotted curve of the fully modified model. The difference in the peak values from these two curves is approximately 10%. If only the viscoelastic material properties are updated (dashed curve), the modified model is not much different from the baseline model (solid curve). Therefore, comparing the fully modified model and the baseline model, we can conclude that the change in the maximum von Mises stress in the brain is mainly caused by the representation of the CSF as hydrostatic fluid cavities, instead of using a solid material definition.

The results of the maximum principal stress in the skull from the sole modification of the CSF definition are shown in Figure 10(A), compared with the results from the baseline model. It is evident that the curves are almost coincident, hence showing that the modification of the

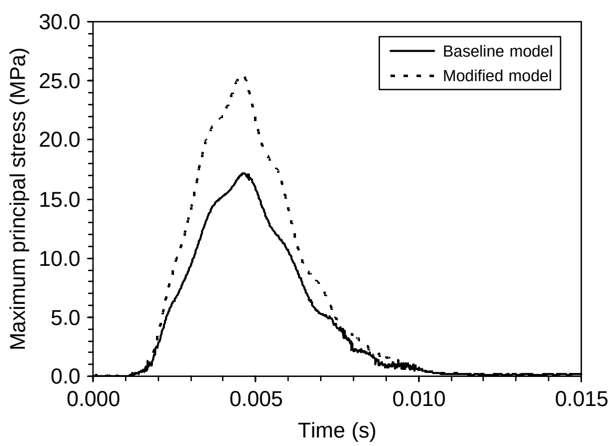

Figure 8. Predictions of the maximum principal stress in the skull during the impact process from the baseline and the modified models.

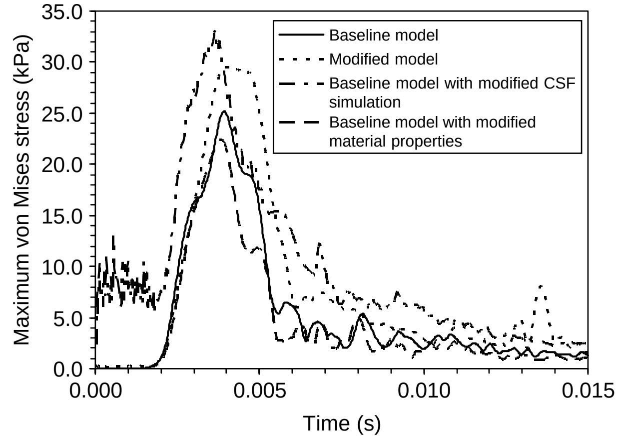

Figure 9. The individual effects of the new CSF simulation and the updated material properties on the maximum von Mises stress in the brain during the impact process, compared with the results from the baseline and the modified models.

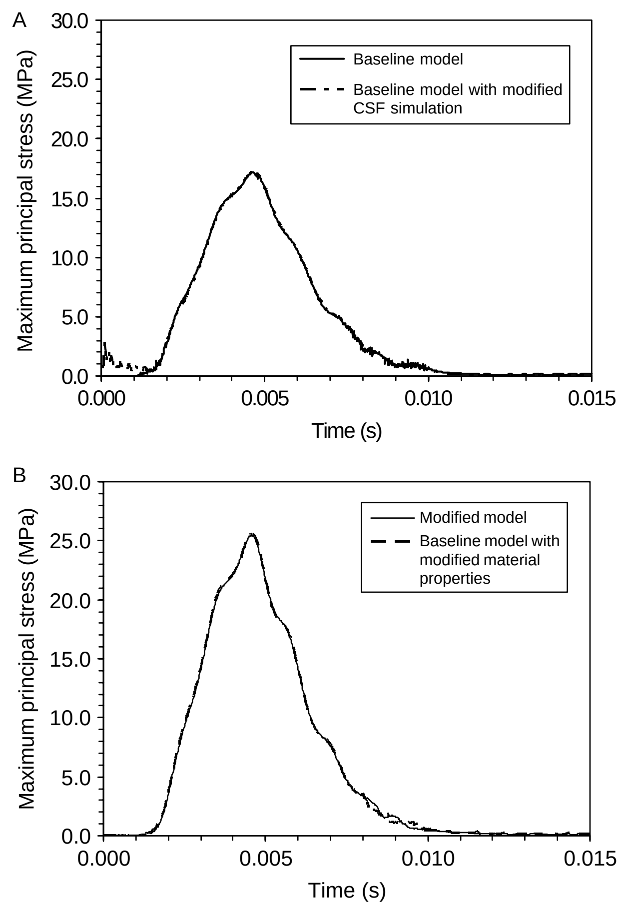

Figure 10. (a) The effect of the modified CSF simulation on the maximum principal stress in the skull during the impact process, compared with the results from baseline model. (b) The effect of the modified material properties on the maximum principal stress in the skull during the impact process, compared with the results from the modified model.

CSF has a negligible effect on the maximum principal stress in the skull. However, if only the viscoelastic properties of the material are updated, the influence is significant, as shown in Figures 8 and 10(B). The maximum principal stress response in the skull resulting from this modification is almost identical to that of the fully modified model. Therefore, it can be concluded that the change in the maximum principal stress in the skull is mainly caused by updating the material properties from linear elasticity to viscoelasticity.

4. Conclusion

Based on Horgan and Gilchrist's (2003, 2004) existing FE head model, a modified numerical model to analyse head impact has been developed. The CSF was simulated as hydrostatic fluid cavities by using a surface-based technique. Except for the scalp, all the head tissues were simulated using viscoelastic materials in the modified model. Theoretically, it was expected that the modified model should improve the accuracy of impact simulation results, when compared to Horgan and Gilchrist's (baseline) model. The modified model predicted a smoother pressure distribution at the coup position without oscillation. When comparing the stresses in the head, the baseline model underestimated the peak von Mises stress in the brain by approximately 15% and the peak principal stress in the head skull by approximately 33%. Furthermore, it was found that the change in the maximum von Mises stress in the brain was mainly caused by the improved CSF material definition (i.e. modelling the CSF as hydrostatic fluid cavities instead of the baseline solid material definition). Similarly, the change in the maximum principal stress in the skull is mainly caused by updating the material properties from linear elasticity to viscoelasticity. Therefore, it was concluded that viscoelasticity of the head tissue should be considered, and that the CSF should be modelled as a fluid instead of a solid, when using FE analysis to study impact head injury.

Acknowledgements

The financial support from the Australian Spitfire Association is acknowledged. This research was undertaken at the NCI National Facility in Canberra, Australia, which is supported by the Australian Commonwealth Government.

References

Abaqus version 6.8, 2008. Dassault Systèmes Simulia Corp., Providence, RI, USA.

Bashkatov AN, Genina AE, Sinichkin YP, Kochubey VI, Lakodina NA, Tuchin VV. 2003. Glucose and mannitol diffusion in human dura mater. Department of Optics, Saratov State University, Saratov, Russia, Vol. 85, p. 3310–3318.

Couper Z, Albermani F. 2007. Infant brain subjected to oscillatory loading: material differentiation, properties, and interface conditions. Biomech Model Mechan. 7:105–125.

Gurdjian E. 1972. Recent advances in the study of the mechanism of impact injury of the head Clin Neurosurg. 19:1–42.

Horgan T. 2005. A finite element model of the human head for use in the study of pedestrian accidents [PhD thesis]. University College Dublin.

Horgan T, Gilchrist M. 2003. The creation of three-dimensional finite element models for simulating head impact biomechanics. Int J Crashworthines. 8:353–366.

Horgan T, Gilchrist M. 2004. Influence of FE model variability in predicting brain motion and intracranial pressure changes in head impact simulations. Int J Crashworthines. 9:401–418.

Kleiven S, Holst HV. 2002. Consequences of head size following trauma to the human head. J Biomech. 35:153–160.

Lakes RS, Katz JL, Sternstein SS. 1979. Viscoelastic properties of wet cortical bone: part I, torsional and biaxial studies. J Biomech. 12:657–678.

Margulies JS, Thibault L, Generalli T. 1985. A study of scaling and head injury criteria using physical model experiments. Paper presented at: Proceedings of 1985 IRCOBI Conference on the Biomechanics of Impacts; Bron, France. p. 223–234.

Marjoux D, Baumgartner D, Deck C, Willinger R. 2008. Head injury prediction capability of HIC, HIP, SIMon and ULP criteria. Accid Anal Prev. 40:1135–1148.

Ma C, Jin X, Zhang J, Huang S. 2008. Development of the pia-arachnoid complex finite element model. Paper presented at: Bioinformatics and Biomedical Engineering, 2008. ICBBE 2008. The 2nd International Conference; Shangai, China. p. 1717–1720.

Nahum A, Smith R, Ward C. 1977. Intracranial pressure dynamics during head impact. Paper presented at: Proceedings of the 21st Stapp Car Crash Conference; Warrendale, PA. SAE Paper 770922. p. 339–366.

Pudenz R, Shelden C. 1946. The lucite calvarium – a method for direct observation of the brain. J Neurosurg. 3:487–505.

Ruan JS, Khalil T, King AI. 1991. Human head dynamic response to side impact by finite element modelling. J Biomech. 113:276–283.

Shuck L, Advani S. 1972. Rheological response of human brain tissue in shear. J Basic Eng. 94:905–911.

Trosseille X, Tarriere C, Lavaste F. 1992. Development of a FEM of the human head according to a specific test protocol. Presented at: Proceedings of the 30th Stapp Car Crash Conference; Warrendale, PA. SAE 235–253.

Willinger R, Kang HS, Diaw B. 1999. Three-dimensional human head finite-element model validation against two experimental impacts. Ann Biomed Eng. 27:403–410.

Yoganandan N, Pintar FA. 2004. Biomechanics of temporo-parietal skull fracture. Clin Biomech. 19:225–239.

Yue X, Wang L, Zhou F. 2008. Amendment on the strain measurement of thin-walled human skull shell as intracranial pressure changes. J Univ Sci Technol Beijing. 15:202–208.

Zhou C, Khalil T, King A. 1995. A new model comparing impact responses of the homgeneous and inhomogeneous human brain. Stapp Car Crash J. 39:121–137.

Zhou C, Khalil T, King A. 1996. Viscoelastic response of the human brain to sagittal and lateral rotational acceleration by finite element analysis. Presented at: Proceedings of the 1996 International IRCOBI Conference on the Biomechanics of Impacts; Dublin, Ireland. p. 35–48.